Chemical Geology 376 (2014) 76–83

Contents lists available at ScienceDirect

Chemical Geology

journal homepage: www.elsevier.com/locate/chemgeo

U–Pb dating of cements in Mesozoic ammonites

Q. Li [a,*], R.R. Parrish [b,c], M.S.A. Horstwood [c], J.M. McArthur [a]

[a] Department of Earth Sciences, UCL, Gower Street, London WC1E 6BT, UK
[b] Department of Geology, University of Leicester, Leicester LE1 7RH, UK
[c] NERC Isotope Geosciences Laboratory, British Geological Survey, Keyworth, Nottingham NG12 5GG, UK

ARTICLE INFO

Article history:
Received 25 September 2013
Received in revised form 26 March 2014
Accepted 31 March 2014
Available online 12 April 2014

Editor: K. Mezger

Keywords:
Mesozoic
Carbonate
Ammonite
Diagenetic
Cement
U-Pb dating

ABSTRACT

Dating sedimentary carbonates using the U-Pb method can help improve the Phanerozoic timescale. Using a novel combination of laser-ablation, multi-collector, inductively-coupled-plasma, mass-spectrometry (LA–MC–ICP–MS) and thermal ionization multi-collector mass spectrometry (TIMS), U-Pb numerical ages were obtained on early-diagenetic calcite cements in Jurassic ammonites in which concentrations of U range from 0.47 to 5.3 ppm.

The calcite cements of two ammonites, IS1 and IS2, from the uppermost *Bifrons* Zone of the Toarcian (179–180 Ma) of the UK, gave TIMS-normalized LA U–Pb dates of 164.9 ± 5.3 Ma and 166.7 ± 4.8 Ma respectively. Normalizing LA–ICP–MC–MS data to an in-house calcite standard gave a more precise date of 165.5 ± 3.3 Ma for IS1 cement. An unzoned ammonite, SS2, of Bajocian age (168–170 Ma) yield a TIMS-normalized LA U–Pb age of 158.8 ± 4.3 Ma for its early-diagenetic cement. Both the combined LA–MC–ICP–MS and TIMS approach, and the use of a calcite laser ablation standard can result in accurate ages of cements with uncertainties of 2–3% (2σ). The later, however, is more efficient and precise. These U-Pb dates of cements are 10 to 20 Myr younger than the numerical ages of the biostratigraphic intervals from which the ammonites derive. The U-Pb dates are taken to represent the time at which the aragonite shell of the ammonite inverted to calcite and released its U to precipitate in a late-diagenetic alteration of early-diagenetic fringing cements.

Concentrations of U and Pb in a range of other pristine biogenic carbonates were found too low (U < 0.01 ppm) for meaningful dating using laser ablation method.

1. Introduction

The feasibility of the Pb-Pb (and so U-Pb) method for dating carbonates was established with apparently meaningful Pb–Pb isochrons for the Archean Mushandike stromatolitic limestone (Moorbath et al., 1987) and the Archean Schmidtsdrif Formation (Jahn et al., 1990) in southern Africa, and with U-Pb dating of coral secondary calcite in Devonian limestones of the Lucas Formation, Ontario (Smith and Farquhar, 1989). Since then U-Pb dating has been applied, with varying robustness, to a range of geological problems through dating of late-diagenetic calcite cements (Smith et al., 1991), early-diagenetic marine carbonate concretions (Israelson et al., 1996), pedogenic calcite (Rasbury et al., 1997), speleothems (Richards et al., 1998), dolomitic hard grounds (Winter and Johnson, 1995), recrystallized biogenic carbonate grainstones (DeWolf and Halliday, 1991), secondary calcite that had inverted from aragonite (Jones et al., 1995; Rasbury et al., 2004), and Pleistocene and Miocene coral aragonite (Getty et al., 2001; Denniston et al., 2008). Reviews by Jahn and Cuvellier (1994) and by Rasbury and Cole (2009) discuss these, and other, examples of such application.

As noted before (e.g. Jones et al., 1995; Israelson et al., 1996), the ability to date sedimentary carbonate rocks using the U–Pb dating method would greatly enhance our ability to calibrate the Phanerozoic timescale. For example, the geological timescale (Gradstein et al., 2012) for the Early and Middle Jurassic Period is calibrated with 19 numerical dates, only one of which derives from Europe where, for this time, the most refined biostratigraphy exists. Direct numerical dating of European sediments would thus improve the tie between numerical and biostratigraphic ages.

Here is reported an attempt to improve the numerical calibration of the geological timescale for Toarcian and Bajocian time by using U-Pb methods to date early diagenetic cements in ammonites of known age. Such ammonites commonly occur well-preserved inside carbonate concretions from Cretaceous and Jurassic mudstones of the UK (Taylor, 1995; Simms et al., 2004). Because they are uncompressed, the ammonites must have been encased in concretionary calcite during very early burial in sediment — probably at depths of no more than a few meters (Marshall, 1981; Raiswell, 1987, 1988; Curtis et al., 2000). The ammonite chambers contain several generations of calcite cements (Marshall, 1981; Curtis et al., 2000) formed under sub-oxic to anoxic

* Corresponding author at: Department of Earth Sciences, Royal Holloway University of London, Egham, Surrey TW20 0EX, UK.
E-mail address: qiong.li@rhul.ac.uk (Q. Li).

http://dx.doi.org/10.1016/j.chemgeo.2014.03.020
0009-2541/

conditions, including an earliest fringing cement that precipitated directly onto the internal walls and septa of the ammonite chambers either before, or immediately on, burial; and a late sparry calcite cement (Fig. 1). It is this early fringing cement that we attempted to date. The original aragonite shell of the ammonites could not be used to date the time of original calcification as it had inverted to calcite after burial.

2. Samples

Measurements of U and Pb concentrations in a range of Mesozoic belemnites, inoceramids, bivalves, ammonites, and diagenetic calcite, showed that only the calcite cements from three ammonite specimens dated here had U–Pb values amenable to dating. For reference, the range of U and Pb concentrations are given in Table 1, while more details of samples are in Appendix 1.

Of the three ammonite specimens suitable for dating, two, IS1 and IS2, were *Hildoceras semipolitum* Buckman (Fig. 1) collected as field finds next to the Hurcott Lane Cutting, near Ilminster, Dorset UK. They derived from the mid-Toarcian Beacon Limestone Formation (p94 of Simms et al., 2004; Boomer et al., 2009) and correlate to the *semipolitum* Horizon of the Submediterranean biostratigraphic scheme of Page (2003). This Horizon correlates to the uppermost subdivision of the *Bifrons* Zone (or Chronozone) of the UK Toarcian (Boomer et al., 2009) and is dated at 178 to 179 Ma (Gradstein et al., 2012). A third ammonite SS2, used for method development because of its excellent quality, was obtained from the collection of the British Geological Survey. The given age was Bajocian (168–170 Ma; Gradstein et al., 2012), but no further details of age or provenance are available.

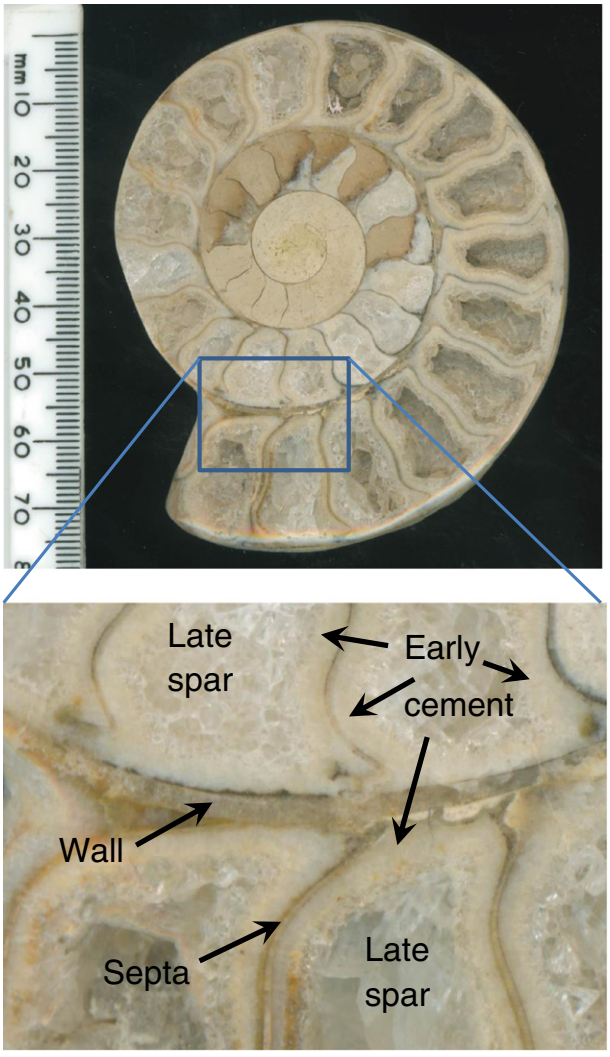

Fig. 1. Specimen IS1 and detail of septa, wall, late spar, and early diagenetic fringing cement that was overprinted during late diagenesis. For explanation, see text. Scale ruler shows unit in millimeters.

Table 1
Summary of U and Pb concentration ranges in various Mesozoic carbonate samples obtained by LA–MC–ICP–MS. Standard zircon 91500 and NIST 614 glass were used as monitors for approximate quantification.

Carbonate sample category	^{238}U ppm	^{206}Pb ppm
Biogenic aragonite	1–8	0.5–19
Belemnite alveolar cement	0.1–0.6	0.3–5.5
Marine concretion cement	0.1	2–10
Biogenic calcite (non-belemnite)	0.02–2.8	0.4
Pristine belemnite calcite	<0.01	<0.04
Altered belemnite calcite	~0.2	~0.02
Ammonite early cement (clean)	0.1–11	0.03–18

Note: there was no attempt to quantify the uncertainty of these rapid screening analyses. These estimates of concentration are indicative only as no calcite standard was available at the time. The detection limit of ^{238}U and ^{206}Pb, was c. 1 ppb.

The fringing cements that have been analyzed by LA–MC–ICP–MS and TIMS are shown in photomicrographs of thin sections in Fig. 2, both in plane-polarized light and with crossed polars. Details of the laser ablation pits and their relation to the cement samples analyzed are shown in Fig. 3.

3. U–Pb methodology

3.1. TIMS analyses

Microsamples of early fringing cements from ammonites (Fig. 1) were obtained using a New Wave Research micromill. The ultrasonically-cleaned sample pieces were completely dissolved in ultrapure 4 N HNO_3 before being spiked with a mixed ^{205}Pb–^{233}U–^{235}U tracer. Following sample-to-spike equilibration, organic matter in samples was destroyed by addition and evaporation of 0.5 ml of concentrated HNO_3 and 0.5 ml H_2O_2. The precipitate was then re-dissolved in 1 ml 1 N HBr for anion exchange chemistry. Eichrom® anion exchange resin (equivalent to BioRad AG 1 - ×8) was used to separate and purify Pb. Uranium was purified using Eichrom UTEVA resin in nitric acid. The purified U and Pb were taken up in 1.2 ml 2% HNO_3 for TIMS analysis. The chemistry blanks were <10 pg for U and <20 pg for Pb.

The U and Pb separates were loaded separately with silica gel and H_3PO_4 onto single outgassed rhenium filaments and analyzed using a Thermo Scientific Triton mass spectrometer fitted with an axial MasCom secondary electron multiplier (SEM) at the NERC Isotope Geosciences Laboratory (NIGL) British Geological Survey, Keyworth, UK. Data were obtained in dynamic single-collector mode on the SEM with Pb and U typically run to exhaustion. Pb and U standards SRM 981 and U500 were analyzed to monitor mass spectrometer performance, ensuring that the SEM linearity, accuracy and reproducibility were better than ±0.1%.

Data reduction, error propagation and plotting were carried out using customized EARTHTIME data reduction spreadsheet following standard parametric statistical methods (Schmitz and Schoene, 2007) and Isoplot version 3.00 (Ludwig, 2003). The decay constants and U isotope composition used were those proposed by Jaffey et al. (1971), as recommended by Steiger and Jager (1977).

3.2. Laser ablation measurements

Laser ablation (LA) analyses were performed using a Nu Plasma HR MC–ICP–MS coupled to a New Wave Research UP193FX (193 nm) excimer laser ablation system. Detection used both Faraday cups and

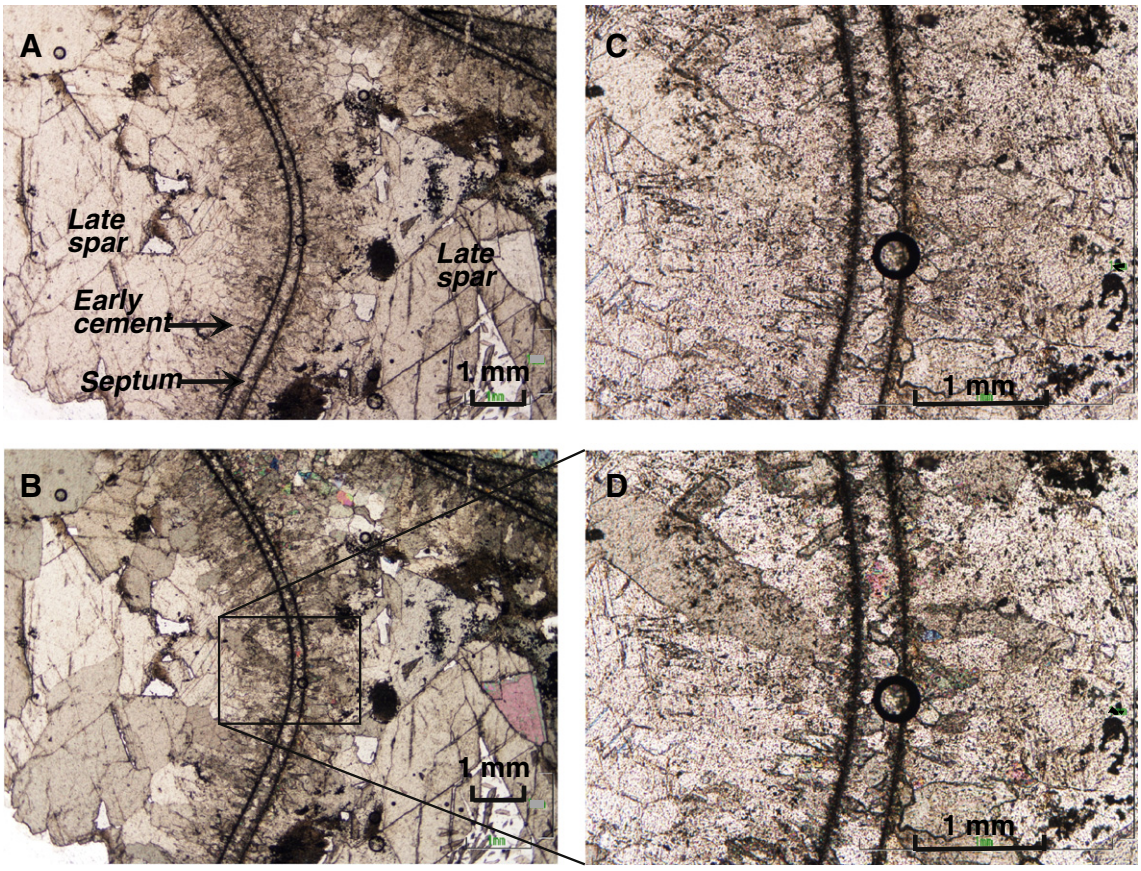

Fig. 2. Photomicrographs of part of IS1, showing septa, early fringing cements (later altered), and late spar. All scale bars 1 mm, with higher magnification on right. Figs. A and C are in plane-polarized light, B and D with crossed polars. Large ring in C and D is a resin bubble; numerous apparent dark inclusions are mostly vugs and pore space.

ion-counting secondary-electron multipliers, with off-line gain calibration. Static ablation used a spot size of 100 μm, a dwell time of 15 s, and a fluence of ~6.7 J/cm^2 at 10 Hz. Prior to measurement, surface Pb contamination was removed by initially ablating to waste for 2 s on each spot. The detection limit for ^{206}Pb was ~1 ppb.

To select samples for analysis, they were analyzed semi-quantitatively for U and Pb concentrations against reference glass NIST 614 or zircon 91500. Isotope ratios were measured on ammonite cement samples for dating. The ^{207}Pb/^{206}Pb ratios were mass bias corrected using NIST 614 or directly normalized to zircon 91500 using the accepted Pb isotope composition (Wiedenbeck et al., 1995). The ^{238}U/^{206}Pb ratios were corrected using the combined TIMS and LA methods described in Section 4.3 for the LA measurements without the concurrent analysis of the in-house calcite standard, and were corrected directly using this calcite standard for IS1 measured along with it. Details of the normalization procedures of the LA data are provided in Appendix 2.

4. Results

4.1. U and Pb concentrations

Concentrations in the ammonite cements obtained by ID-TIMS (Table 2) range up to 5.3 ppm for U and up to 2.1 ppm for Pb. The intensity-derived indicative concentrations by LA–ICP–MC–MS range up to 11 ppm for U and up to 18 ppm for Pb (Table 1, see also Appendices 3–4). These U and Pb concentrations vary by a factor of ≥100 and in part indicate that some subsamples have relatively high radiogenic Pb.

The concentrations of U and Pb in Mesozoic sample categories by LA–MC–ICP–MS are shown in Table 1. Fossil ammonite nacre (aragonite) and most marine diagenetic calcite are subject to common Pb incorporation during diagenesis. Pristine biogenic calcite generally has U and Pb at ppb level.

4.2. TIMS U–Pb ratios and ages

The ^{238}U/^{206}Pb ratios of the cements obtained by TIMS fall in a range of 3.3–19, and the ^{207}Pb/^{206}Pb ratios vary from 0.46 to 0.77 (Table 2). The TIMS data alone give U-Pb ages of 156.2 ± 4.8 Ma (MSWD = 0.68), 170 ± 11 Ma (MSWD = 10.8), and 171 ± 16 Ma (MSWD = 0.51) for cement samples from SS2, IS2 and IS1, respectively (Fig. 4). These ages, although accurate, are not as precise as data obtained by LA analysis owing to the more limited spread in U–Pb ratios. In order to improve the statistics of the TIMS regressions, the TIMS data were anchored by common lead composition (^{207}Pb/^{206}Pb = 0.83 ± 0.01), which was determined from the ^{207}Pb/^{206}Pb intercepts on Tera–Wasserburg plots of LA data, and is shown in the blue boxes in Fig. 4. Using this approach, numerical ages derived from anchored-TIMS data (Fig. 4) are 156.2 ± 4.8 (MSWD = 0.45) for SS2, 170.4 ± 9.0 (MSWD = 8.6) for IS2, and 171 ± 16 (MSWD = 0.34) for IS1, all of which have smaller MSWD than ages from non-anchored TIMS data. These ages are ~10 Ma younger than the corresponding biostratigraphic ages of the fossils.

4.3. LA–ICP–MC–MS U–Pb ratios and ages

The measured LA–MC–ICP–MS U–Pb data need correction for inter-element fractionation on ^{238}U/^{206}Pb ratios, due to matrix difference between calcite samples and standards (NIST glass 614 and zircon 91500), but it demonstrates coherent Tera–Wasserburg (T–W) regressions extrapolating to a common Pb (^{207}Pb/^{206}Pb) composition of 0.83 ± 0.01, implying system behavior that is close to being closed. The inter-

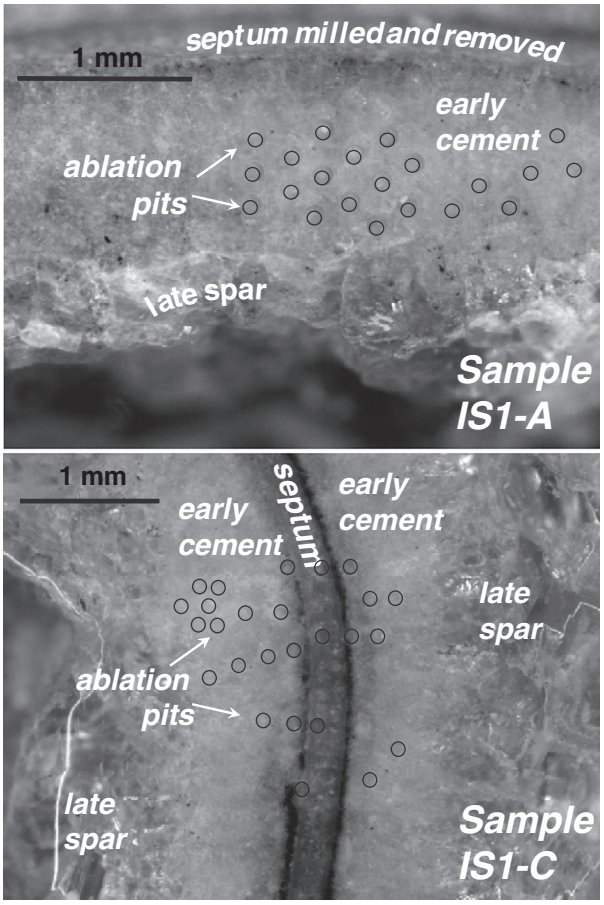

Fig. 3. Photomicrographs of ablated cements showing two chambers A and C of ammonite IS1. Upper figure shows early cement and later spar of IS1-A and analyzed ablation pits within the early cement after removal of the septum by milling. Lower figure shows sample IS1-C with calcite septum inverted from aragonite, altered early-cement, late spar, and ablation pits. All pits gave data consistent with the pooled age.

element fractionation factors were derived by ratioing the $^{238}U/^{206}Pb$ axial-intercept on the anchored-TIMS regressions (Fig. 4) to the $^{238}U/^{206}Pb$ axial-intercept on the LA data arrays (not shown). The inter-element fractionation factors vary with matrix, ablation parameters, and instrument conditions, and are presented in Appendix 2. The corrected LA $^{238}U/^{206}Pb$ ratios range up to 39 and $^{207}Pb/^{206}Pb$ ratios range from 0.11 to 0.83 (Fig. 5). Ages and 2σ uncertainties obtained for SS2, IS2, and IS1, are 158.8 ± 2.6 (±4.3 external uncertainty including quadratic addition of external anchored TIMS uncertainty of 2%), 166.7 ± 3.3 (±4.8 external uncertainty), 164.9 ± 2.1 (±5.3 external uncertainty), with MSWDs of 1.5–4.5 (Fig. 5). The lower uncertainties compared to those derived from anchored TIMS isochrons reflect the greater spread in U–Pb ratios for the LA data. Ages derived by each method are summarized in Table 3, with input data in Appendices 3–4.

The inter-element fractionation on U–Pb ratios during LA analysis can also be countered by analysis of a calcite standard of known age in tandem with the calcite sample being dated. Sample IS1 was therefore also dated by LA–ICP–MC–MS using an in-house U–Pb carbonate reference material with a TIMS age of 251 ± 2 Ma (E.T. Rasbury, pers. comm. 2013). The normalization used similar methods to those described but it was done by correcting (normalizing) the measured array of the calcite standard to intersect the Concordia at 251 Ma and correcting all IS1 data by this same factor (see Appendix 2). The data on standard, IS1 cement, NIST 614 glass (used for lead isotope normalization), and zircon 91500 are all shown in Appendix 4 and Fig. 6. The standard reproduces to 250.4 ± 2.7 (MSWD = 1.7) and the calcite standard-normalized LA–MC–ICP–MS age of IS1 cement is 165.5 ± 3.3 Ma with MSWD of 1.6 (Fig. 6, Table 3), the uncertainty includes the quadratic addition of 1% uncertainty in the age of 251 Ma for the calcite standard.

5. Discussion

5.1. U-Pb dating methodology

This study shows that well preserved biogenic, low-Mg belemnite calcite, contains <0.01 ppm of U and <0.04 ppm of Pb, making it unsuitable for dating by either isotope dilution or laser ablation approaches. Low concentrations of U and radiogenic Pb (and so low U–Pb ratios) in most natural carbonates, and the need for high precision results, have dictated the use of bulk sampling in U–Pb dating. Bulk sampling serves to homogenize small-scale variation, limit the observed range in U–Pb ratios, and so degrade the quality of the dating. As implied by Moorbath et al. (1987), decreasing sample size in carbonates may increase the spread of U–Pb isotopic ratios and so lead to better constrained isochrons and so better ages.

Previous work on sedimentary calcite has used sample sizes of milligrams and more, and samples with high concentrations of U, typically tens of μg/g or more, and a high proportion of radiogenic Pb (i.e. with high $^{238}U/^{204}Pb$ ratios). The use of laser-ablation (LA) for sampling as done here, with spot sizes of around 100 μm in diameter, has exploited the potential for small-scale heterogeneity in carbonates. The samples were typically no more than 1 microgram in mass, a sample size around 1000 times smaller than usual with bulk sampling. In addition, the potential for LA sampling of sedimentary calcite with low concentrations of U (up to 10 ppm U) is shown here. Our data demonstrates the feasibility of dating marine calcite cements using LA–ICP–MC–MS.

A comparison of LA-derived data with TIMS data shows the increased spread on isochrons obtainable with LA sampling. The LA–MC–ICP–MS data produce coherent arrays of much larger variation in

Table 2
U–Pb data of the early cements IS1, IS2 and SS2 by ID-TIMS.

Sample	Wt. mg	U ppm	Pb ppm	Pb (pg)	$^{238}U/^{206}Pb$	2σ (%)	$^{207}Pb/^{206}Pb$	2σ (%)	$^{204}Pb/^{206}Pb$	2σ (%)	Corr. coef. 8/6–7/6	Corr. coef. 8/6–4/6	Corr. coef. 7/6–4/6
IS2 A-d2-1	7.7	3.30	0.689	4687	12.48	0.57	0.5820	0.24	0.03615	0.26	−0.29	−0.28	0.31
IS2 A-d2-2	6.9	2.68	0.549	3354	12.79	0.6	0.5840	0.19	0.03627	0.23	−0.64	−0.56	0.88
IS2 A-d2-3	6.9	2.65	0.577	3547	12.18	0.5	0.5941	0.18	0.03694	0.21	−0.73	−0.66	0.88
IS2 A-d4	5.0	3.35	0.630	2738	13.57	0.6	0.5605	0.25	0.03471	0.30	−0.80	−0.72	0.90
IS2 A-d2-3 Re	6.9	2.65	0.579	3556	12.14	0.5	0.5944	0.17	0.03692	0.21	−0.74	−0.66	0.88
IS2 A-d2	8.0	5.31	0.720	4755	17.04	0.4	0.4887	0.30	0.02974	0.27	−0.36	−0.43	0.43
IS1 AO-e2	5.8	1.96	1.901	10,730	3.32	0.4	0.7710	0.08	0.04897	0.09	−0.12	−0.08	−0.06
IS1 AO-e3	9.4	1.94	1.861	17,123	3.35	0.4	0.7708	0.19	0.04887	3.96	−0.12	0.01	−0.02
IS1 AO-f2	6.4	2.08	1.490	9248	4.39	0.4	0.7484	0.32	0.04732	0.23	−0.10	0.09	−0.16
IS1 AO-f3	3.7	2.32	2.095	7494	3.54	0.4	0.7655	0.25	0.04846	0.31	−0.14	0.04	−0.16
SS2 A-c6	1.6	0.99	0.120	155	18.58	2.6	0.4623	1.21	0.02814	1.32	−0.53	−0.52	0.98
SS2 A-c1	5.4	0.83	0.190	927	11.57	0.5	0.5990	0.16	0.03750	0.21	−0.57	−0.26	0.17
SS2 A-c1 Re	5.4	0.83	0.190	924	11.58	0.5	0.5992	0.16	0.03743	0.21	−0.57	−0.26	0.18
SS2 A-c2	3.7	0.47	0.062	194	17.63	1.2	0.4868	0.91	0.02987	0.99	−0.98	−0.95	0.96

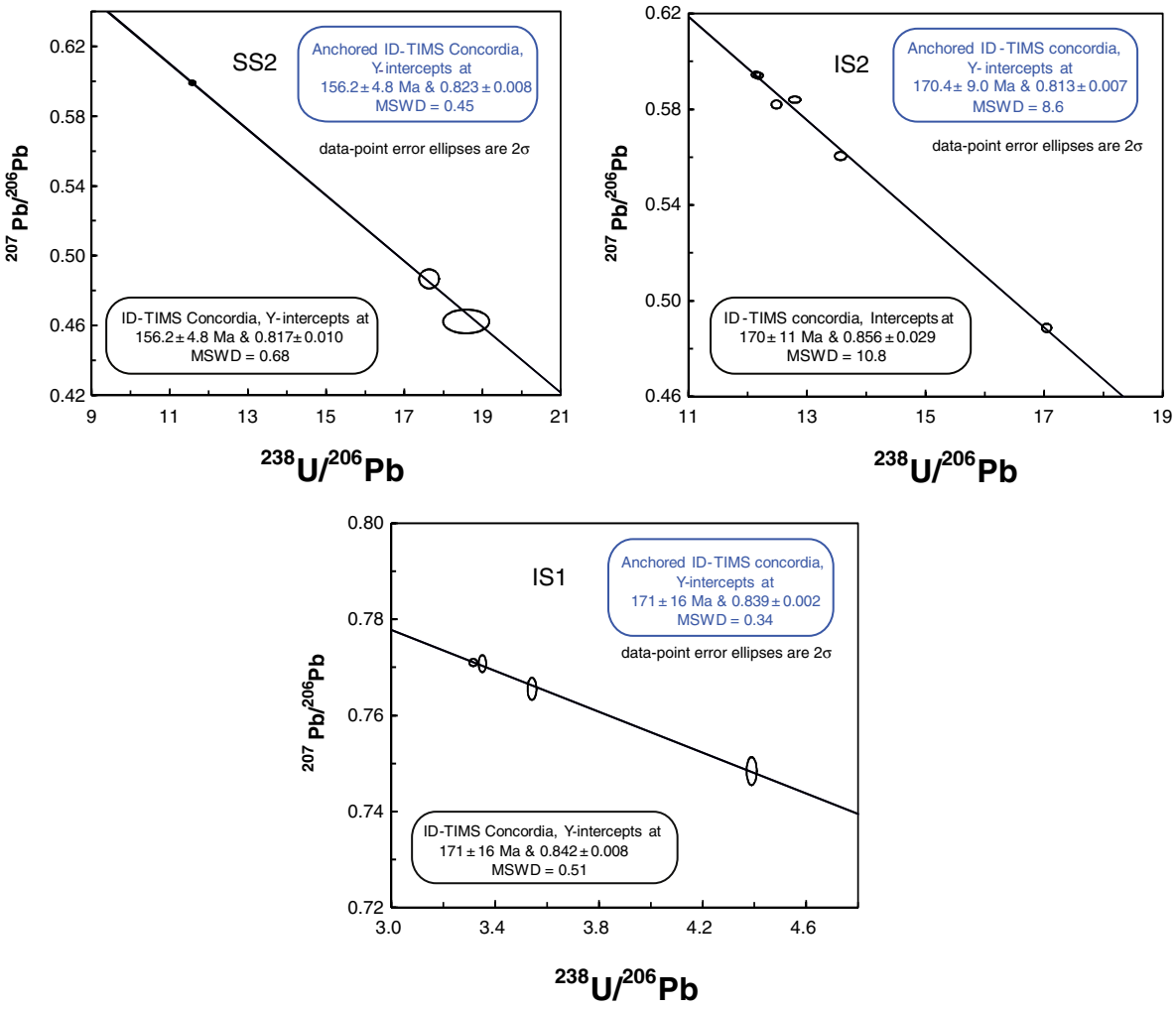

Fig. 4. Tera–Wasserburg Concordia diagrams for samples (a) SS2; (b) IS2 and (c) IS1 showing regressions for TIMS U–Pb data (black line and legend), and for TIMS data anchored using a common Pb isotope ratio of 0.83 ± 0.01 derived from the LA–ICP–MC–MS in Fig. 3 (blue legend and line, the latter hidden beneath the black regression line). Errors are shown at 2σ. Neither axes start from 0 in order to better see the data ellipse in the diagrams; the Concordia curve plots outside of the axial ranges shown.

U–Pb ratios than did microdrilling for TIMS analysis (Table 2, Figs. 4–6 and Appendices 3–4). Provided that an inter-element and lead isotope fractionation corrections are made, LA–MC–ICP–MS U–Pb isotope data can provide an accurate determination of both common Pb (initial $^{207}Pb/^{206}Pb$) and reliable U–Pb ratios on a very small (≤50 μm) scale in the low-U carbonates. Such corrections were made here using ID-TIMS, by the use of NIST 614 glass, Zircon 91500, and by the use of a calcite reference material in combination with LA methods.

Either the use of a calcite laser ablation reference material of known age, or the combined LA- and TIMS analysis on at least moderately radiogenic portions of such carbonate samples, normalizes sufficiently well to yield accurate LA–MC–ICP–MS U–Pb data that gives LA U–Pb cement ages with 2σ uncertainties as little as 2–3%. The use of a calcite reference, however, is more efficient because it eliminates the need for any TIMS analysis and, for example, allows an analysis to be completed within 4 h. These two approaches are potentially useable in time scale calibration in the absence of high precision Ar–Ar or U–Pb ages of volcanic materials from ash beds, or in studies of the chronology of diagenesis and pore filling in sedimentary rocks.

5.2. Interpretation of U–Pb ages

The small scatter in both LA-derived and TIMS-derived data suggests that the U–Pb system in our samples is not perfectly closed. Nevertheless, the scatter is sufficiently small for the derived ages to have acceptably high precision and low MSWD, and lends confidence to our view that the derived ages are meaningful.

Samples IS1 and IS2 are from the uppermost *Bifrons* Zone of the Toarcian. This interval has a numerical age of 179 to 180 Ma (Gradstein et al., 2012). The numerical ages of ammonite cements obtained here are close to 165 Ma, some 15 Myr younger. The specimen SS2 is of Bajocian age, which spans the interval 168.3 to 170.3 Ma (Gradstein et al., 2012). The SS2 has a U–Pb cement age of 159 Ma, some 10 Myr younger than its Bajocian depositional age.

These measured ages are interpreted to be the time at which the walls, septa, and early-diagenetic fringing cements of the analyzed ammonites inverted from aragonite to calcite and distributed their U into the early-diagenetic fringing cements as they recrystallized during late diagenesis.

The internal cements of ammonites from Jurassic concretions were studied in detail by both Marshall (1981) and by Curtis et al. (2000). Both authors note multiple generations of cements, and both recognized that the first cement deposited was an acicular, fringing, cement that precipitated directly onto septa and walls of the original organism. Both agree the cement is very early diagenetic. Marshall (1981) however, recognized petrographically that this early cement was overprinted by a later diagenetic modification that introduced cloudiness to the original cement textures. A similar cloudiness is seen in the cements

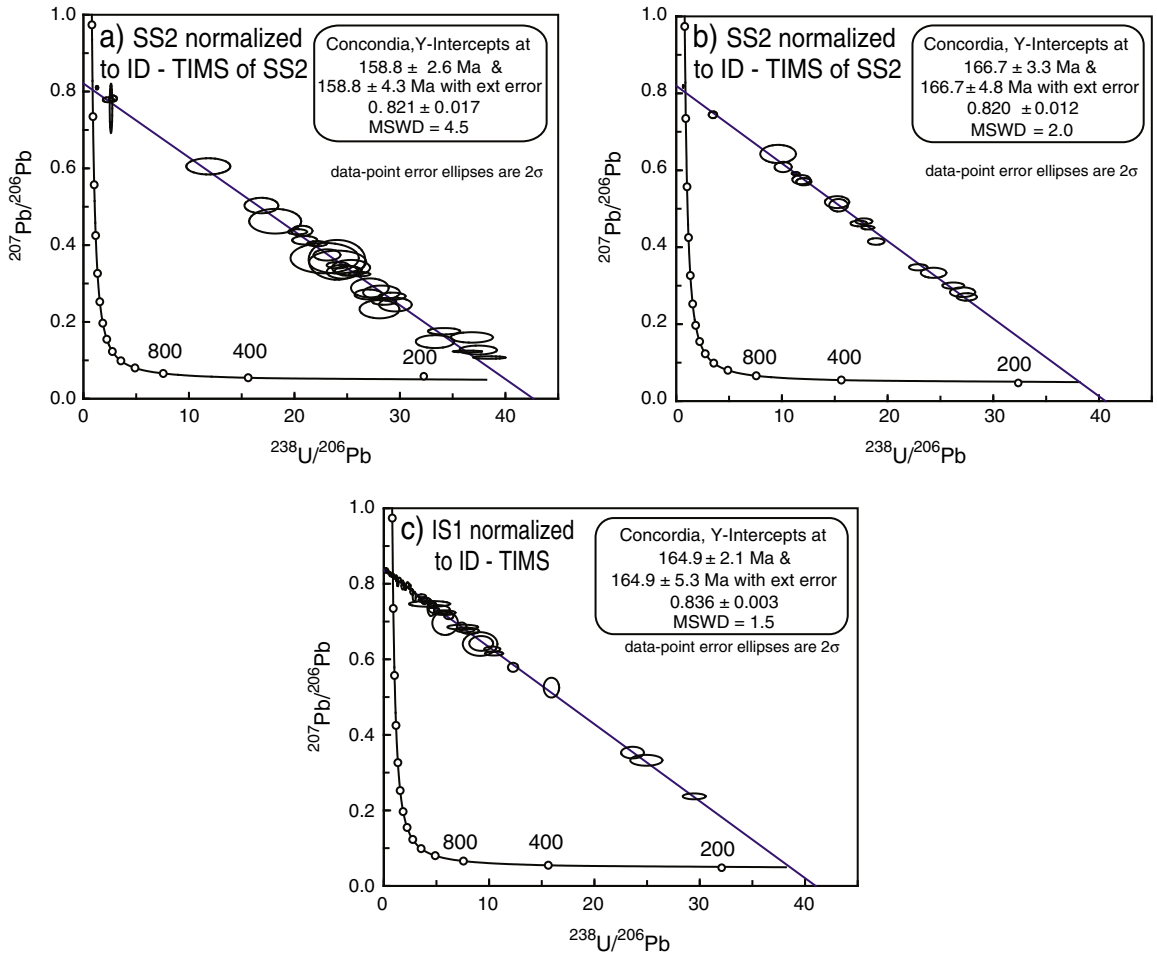

Fig. 5. Tera–Wasserburg Concordia diagrams of LA–ICP–MC–MS U–Pb data that has been normalized to TIMS measurements. LA data of samples (a) SS2 and (b) IS2 has been normalized to TIMS data of SS2, and LA data of (c) IS1 to TIMS data of IS1, respectively. Error ellipses are shown at 2σ. External errors reflect the quadratic addition of the external uncertainty of the common-lead-anchored TIMS ages of samples SS2 and IS1, as described in the text and Appendix 2.

fringing the walls and septa of the analyzed ammonites (Figs. 1–3). Our dating identifies the timing of the late diagenetic alteration of the early cements as occurring between 10 Myr (SS2) and 15 Myr (IS1, IS2) after formation of the original cement. The U in the cloudy, now altered, fringing cements was, we postulate, mobilized from inverting aragonite in septa and walls of the original ammonite shells. A similar incorporation of U into calcite cements from recrystallizing aragonite was noted by Jones et al. (1995) in secondary calcite cements after aragonite in the Permian Reef Complex of New Mexico.

Table 3
Tera–Wasserburg age regression results for LA–MC–ICP–MS and ID-TIMS data of cements SS2, IS2 and IS1 and calcite standard-normalized LA–MC–ICP–MS data for IS1 (ccstd). All ages are reported in Ma at 2σ. External errors include quadratic addition of the 2% uncertainty of the anchored ID-TIMS regression used for normalization.

Samples		SS2	IS2	IS1
ID-TIMS	Age	156.2	170	171
	2σ	4.8	11	16
	MSWD	0.68	10.8	0.51
LA–MC–ICP–MS anchored ID-TIMS	Age	156.2	170.4	171
	2σ	4.8	9.0	16
	MSWD	0.45	8.6	0.34
ID-TIMS corrected LA–MC–ICP–MS	Age	158.8	166.7	164.9
	2σ	2.6	3.3	2.1
	2σ external	4.3	4.8	5.3
	MSWD	4.5	2.0	1.5
Calcite std corrected LA–MC–ICP–MS	Age	/	/	165.5
	2σ	/	/	3.3
	MSWD	/	/	1.6

5.3. Reassessing published U/P ages on sedimentary calcite

Given that our dating shows a strong discordance between depositional and diagenetic ages, it seems worthwhile briefly to re-examine dates obtained on carbonates in the past, where a degree of concordance between depositional and measured diagenetic ages was commonly asserted.

A U–Pb isochron age of 249.8 ± 4.7, was obtained by Jones et al. (1995) for calcite, inverted from aragonite in Uppermost Capitan Formation, Guadalupian Epoch, Late Permian. The age of this unit is now considered to be around 260 to 262 Ma (Gradstein et al., 2012), suggesting that the inversion occurred around 10 Myr after initial deposition of the aragonite, rather than close to the time of deposition, as reported by Jones et al. (1995).

A calcareous concretion from the upper part of the *Peltura scarabaeoides* Zone (Late Cambrian) of the Alum Shale of southern Sweden, yielded a Pb/Pb age of 509.8 ± 5.1 Ma (Israelson et al., 1996). These authors proposed that it represents the time of diagenetic growth during the first few meters of burial. According to Gradstein et al. (2012), the *Ctenopyge bisulcata* Subzone, which was the lowest subzone of the (now abandoned) *P. scarabaeoides* Zone, occurs in the uppermost Furongian and has a maximum age of 489 ± 3 Ma. This disparity of age suggests that the Pb/Pb age is not recording the time of concretion formation. Apparently from the same Alum shale locality, a calcareous

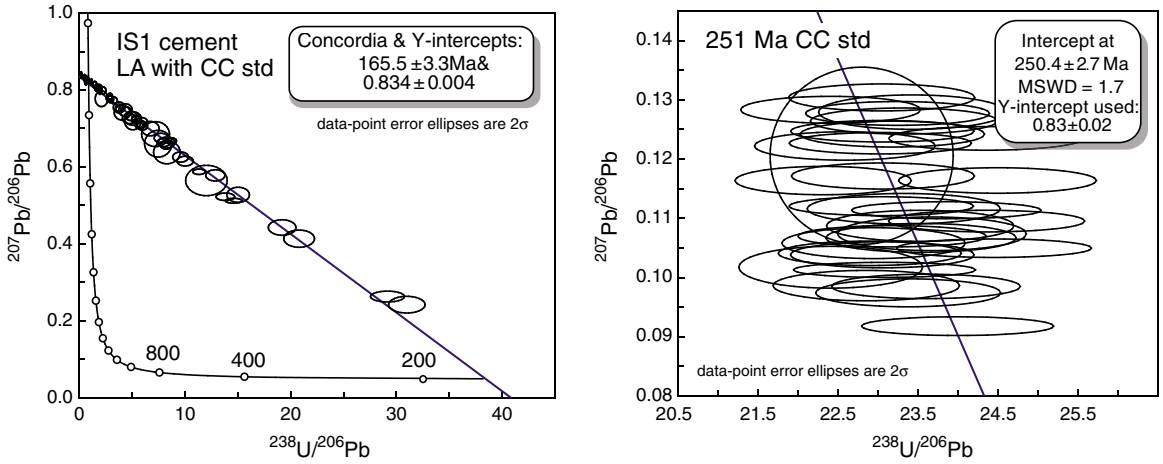

Fig. 6. Tera–Wasserburg Concordia diagrams for LA–MC–ICP–MS U–Pb data of sample IS1 (left) normalized to the 251 ± 2 Ma calcite U–Pb standard (right), as described in the text. Error ellipses are shown at 2σ. The calcite standard data is an expanded view showing the coherence of the data; small variation in $^{207}Pb/^{206}Pb$ reflects variable proportions of common lead admixed with radiogenic lead.

cone-in-cone structure, believed to represent late-diagenetic growth, yielded a Pb/Pb age of 478.2 ± 4.9. The age of this calcite is around 10 Myr younger than the age of the enclosing sediment, as is appropriate for a late-diagenetic structure.

Calcite, inverted from aragonite cements, a few meters below the Carboniferous/Permian boundary in the latest Carboniferous Laborcita Formation of New Mexico (Rasbury et al., 2004) yielded an age of 300.2 ± 3.8 which is in concordant with the most recent estimate of 298.9 Ma for the age of that boundary given in Gradstein et al. (2012).

These comparisons suggest that care is needed in interpreting cement ages, and that they cannot be reliably assumed to be early diagenetic; that is, formed within a few hundred, a few thousand, or even a few hundred thousand years of the depositional age of the enclosing sediment. The U-Pb results given here can provide a more robust understanding of the chronology of diagenetic processes in carbonates. This paper confirms that early cements in ammonites may have later diagenetic overprints, as proposed long ago by Marshall (1981).

6. Conclusions

(1) Pristine biogenic calcite contains <0.01 ppm of U, making it unsuitable for U–Pb dating with the sensitivity presently attainable with TIMS or ICP–MC–MS.
(2) Two methods of analysis yield precise U–Pb dates for early diagenetic calcite cements: LA–MC–ICP–MS analysis normalized to TIMS analysis of the same sample to remove U–Pb inter-element fractionation during LA analysis; LA–ICP–MC–MS analysis concurrently with a calcite reference of known age. This later method is rapid, more precise (2% 2σ) and recommended for future use in U–Pb dating of calcite.
(3) Early-diagenetic calcite cements in ammonites preserved within concretionary carbonates may be overprinted during late diagenesis (e.g. 10–20 Myr after original cement formation) and incorporate U and Pb from the recrystallizing aragonite of the original shell and septa of the organism. Good isochrons derived from such material record the time of overprinting and aragonite inversion to calcite, rather than the time of precipitation of the early-diagenetic fringing cements on ammonite septa and walls.

Supplementary data to this article can be found online at http://dx.doi.org/10.1016/j.chemgeo.2014.03.020.

Acknowledgments

The authors thank Nick Roberts, Daniel Condon, Nicola Atkinson, Wendy Austin-Giddings and Steve Noble for assistance in the acquisition of analytical data at the NERC Isotope Geosciences Laboratories. Kevin Page is also thanked for ammonite identification.

References

Boomer, I., Lord, A., Page, K., Bown, P., Lowry, F., Riding, J.B., 2009. The biostratigraphy of the Upper Pliensbachian–Toarcian (Lower Jurassic) sequence at Ilminster, Somerset. J. Micropalaeontol. 28, 67–85.
Curtis, C.D., Cope, J.C.W., Plant, D., Macquaker, J.H.S., 2000. 'Instantaneous' sedimentation, early microbial sediment strengthening and a lengthy record of chemical diagenesis preserved in Lower Jurassic ammonitiferous concretions from Dorset. J. Geol. Soc. 157, 165–172.
Denniston, R.F., Asmerom, Y., Polyalk, V.Y., McNeill, D.F., Klaus, J.S., Cole, P., Budd, A.F., 2008. Caribbean chronostratigraphy refined with U–Pb dating of a Miocene coral. Geology 36, 151–154.
DeWolf, C.P., Halliday, A.N., 1991. U–Pb dating of a remagnetized Paleozoic limestone. Geophys. Res. Lett. 18, 1445–1448.
Getty, S.R., Asmerom, Y., Quinn, T.M., Budd, A.F., 2001. Accelerated Pleistocene coral extinctions in the Caribbean Basin shown by uranium–lead (U–Pb) dating. Geology 29, 639–642.
Gradstein, F.M., Ogg, J.G., Schmitz, M.D., Ogg, G.M., 2012. The Geologic Time Scale 2012, 2-Volume Set, Volume 2. Elsevier BV, 1176 p.
Israelson, C., Halliday, A.N., Buchardt, B., 1996. U–Pb dating of calcite concretions from Cambrian black shales and the Phanerozoic time scale. Earth Planet. Sci. Lett. 141, 153–159.
Jaffey, A.H., Flynn, K.F., Glendeni, Le, Bentley, W.C., Essling, A.M., 1971. Precision measurement of half-lives and specific activities of ^{235}U and ^{238}U. Phys. Rev. C 4, 1889–1906.
Jahn, B.M., Cuvellier, H., 1994. Pb–Pb and U–Pb geochronology of carbonate rocks: an assessment. Chem. Geol. 115, 125–151.
Jahn, B.-M., Bertrand-Sarfati, J., Morin, N., Mace, J., 1990. Direct dating of stromatolitic carbonates from the Schmidtsdrif Formation (Transvaal Dolomite), South Africa, with implications on the age of the Ventersdorp Supergroup. Geology 18, 1211–1214.
Jones, C.E., Halliday, A.N., Lohmann, K.C., 1995. The impact of diagenesis on high-precision U–Pb dating of ancient carbonates — an example from the Late Permian of New-Mexico. Earth Planet. Sci. Lett. 134, 409–423.
Ludwig, K.R., 2003. User's Manual for Isoplot 3.00. Berkeley Geochronology Center, Berkeley, CA.
Marshall, J.D., 1981. Zoned calcites in Jurassic ammonite chambers: trace elements, isotopes and neomorphic origin. Sedimentology 28, 867–887.
Moorbath, S., Taylor, P., Orpen, J., Treloar, P., Wilson, J., 1987. First direct radiometric dating of Archaean stromatolitic limestone.
Page, K.N., 2003. The Lower Jurassic of Europe: its subdivision and correlation. Geol. Surv. Denmark Greenland Bull. 1, 23–59.
Raiswell, R., 1987. Non-steady state microbiological diagenesis and the origin of concretions and nodular limestones. Geol. Soc. Lond., Spec. Publ. 36, 41–54.
Raiswell, R., 1988. Chemical model for the origin of minor limestone-shale cycles by anaerobic methane oxidation. Geology 16, 641–644.
Rasbury, E.T., Cole, J.M., 2009. Directly dating geologic events: U–Pb dating of carbonates. Rev. Geophys. 47, RG3001.

Rasbury, E., Hanson, G., Meyers, W., Saller, A., 1997. Dating of the time of sedimentation using U–Pb ages for paleosol calcite. Geochim. Cosmochim. Acta 61, 1525–1529.
Rasbury, E.T., Ward, W.B., Hemming, N.G., Li, H., Dickson, J.A.D., Hanson, G.N., Major, R.P., 2004. Concurrent U–Pb age and seawater $^{87}Sr/^{86}Sr$ value of a marine cement. Earth Planet. Sci. Lett. 221, 355–371.
Richards, D.A., Bottell, S.H., Cliff, R.A., Strohle, K., J. R.P., 1998. U–Pb dating of a speleothem of Quaternary age. Geochim. Cosmochim. Acta 62, 3683–3688.
Schmitz, M.D., Schoene, B., 2007. Derivation of isotope ratios, errors, and error correlations for U–Pb geochronology using Pb-205–U-235–(U-233)-spiked isotope dilution thermal ionization mass spectrometric data. Geochem. Geophys. Geosyst. 8, 1–20.
Simms, M.J., Chidlaw, N., Morton, N., Page, K.N., 2004. British Lower Jurassic Stratigraphy. Geological Conservation Review Series, No. 30, Joint Nature Conservation Committee, Peterborough (458 pp.).
Smith, P.E., Farquhar, R.M., 1989. Direct dating of Phanerozoic sediments by the ^{238}U–^{206}Pb method. Nature 341, 518–521.
Smith, P.E., Farquhar, R.M., Hancock, R.G., 1991. Direct radiometric age-determination of carbonate diagenesis using U–Pb in secondary calcite. Earth Planet. Sci. Lett. 105, 474–491.
Steiger, R.H., Jager, E., 1977. Subcommission on geochronology — convention on use of decay constants in geochronology and cosmochronology. Earth Planet. Sci. Lett. 36, 359–362.
Taylor, P.D., 1995. Field Geology of the British Jurassic. Geological Society Pub House pp. 105–150.
Wiedenbeck, M., Alle, P., Corfu, F., Griffin, W., Meier, M., Oberli, F., Quadt, A.V., Roddick, J., Spiegel, W., 1995. Three natural zircon standards for U–Th–Pb, Lu–Hf, trace element and REE analyses. Geostand. Newslett. 19, 1–23.
Winter, B.L., Johnson, C.M., 1995. U–Pb dating of a carbonate subaerial exposure event. Earth Planet. Sci. Lett. 131, 177–187.